ESCUELA DE CONSTRUCCIÓN CIVIL
FACULTAD DE INGENIERÍA

Revista de la Construcción
Journal of Construction

Research Article

Compressive resistance level effect on impact performance of fiber reinforced concrete

Juan Carlos Vivas[1]*, **Raúl Zerbino**[1]

[1] CONICET. LEMIT and Faculty of Engineering UNLP, Buenos Aires (Argentina)
*Correspondence: juancarlos.vivas@ext.ing.unlp.edu.ar

Received: 22.03.2021; **Accepted:** 03.03.2021; **Published:** 18.04.2022

Citation: Vivas, J. and Zerbino, R. (2022). Compressive Resistance Level Effect on Impact Performance of Fiber Reinforced Concrete. Revista de la Construcción. Journal of Construction, 21(1), 135-144. https://doi.org/10.7764/RDLC.21.1.135.

Abstract: impact resistance represents a key property of fiber reinforced concrete (FRC). To study this property, a test method was recently proposed; which consists in repeated drops of a projectile on simply supported prisms, and allows to evaluate FRC behavior both at cracking and after cracking. With the aim of verifying the sensitiveness of this method, this paper analyzes the influence of the compressive strength of the FRC matrix on each parameter of the impact test. Three FRC incorporating 30 kg/m^3 of hooked-end steel fibers were prepared, varying the water/cement ratio (0.59, 0.50 and 0.43). It was found that although only small effects on the cracking energy were observed as the concrete compressive strength increases, the post-cracking energy increased in a greater proportion. However, the cracking growth rate, an impact parameter strongly sensitive to the type and content of fibers, remained practically constant for different compressive strength levels.

Keywords: fiber reinforced concrete, compressive resistance, steel fibers, drop-weight impact test, residual strength.

1. Introduction

Almost since its appearance, the good impact resistance presented in the Fiber Reinforced Concrete (FRC) has been evident; so much that the ACI 544 Committee (ACI Committee 544, 1999, 2017) and many authors (Sateshkumar et al., 2018; Ulzurrun & Zanuy, 2017; Yu, Van Beers, Spiesz, & Brouwers, 2016) has highlight it as one of the main properties of this compound. Nevertheless, the study the impact resistance has great challenges; first, due to this phenomenon complexity, since the stress application occurs in very short time and loads magnitude very variables can be reached; but also, because there is not a widely accepted test method that allows to evaluate the variables affecting the impact resistance of FRC, as the type and content of fibers. This becomes relevant as, in last time, the industry of fibers for concrete has experienced an accelerated evolution.

This issue is very important for engineering since many structures are subjected on impact actions; among them: pavements, piles and many highway accessories, security and defense structures, soil support structures, such as walls and tunnels, which are not only exposed to impacts in the service but also during the construction. For that reason, a project has been undertaken with the purpose of characterize the FRC under impacts and understand the influence of different variables, both those of the test as the material. An advantage of this test is that the impact performance of FRC is evaluated distinguishing two phases: up to cracking (Phase 1) and after cracking (Phase 2), given as results various impact parameters for each one of them. It has been widely recognized that the main contribution of the fibers take place in cracked state.

In previous research, the effect of type and content of fiber has been studied (Juan C. Vivas, Zerbino, Torrijos, & Giaccio, 2020a). In that work, six FRC were prepared with the same base (plain) concrete, incorporating different dosages of steel (25 and 50 kg/m^3), alkali-resistant glass (6 and 12 kg/m^3) and polymeric (5 and 10 kg/m^3) macrofibers. Although all fibers improved the impact performance of concrete, different behaviors between each FRC were observed. Regarding the behavior before cracking, in all cases was found that the cracking energy was practically constant for all FRC, which suggested that this property mainly depends on matrix characteristics (i.e., compressive strength). On the contrary, other parameters, like the post cracking energy and total energy strongly varied between each FRC, verifying that these parameters depend on the type and fiber content. Similarly, he cracking growth rate (V_C), other proposed post cracking parameter, exhibited great sensitivity to type and content of fibers, as it is related to the action mechanism of each fiber.

In other paper (Juan C. Vivas, Zerbino, Torrijos, & Giaccio, 2020b), the effect of the class of FRC following the proposal of the *fib* Model Code 2010 (International Federation for Structural Concrete (*fib*), 2012) were compared. In this case FRC with a similar residual stress f_{R1}, measured at crack mouth opening displacement (CMOD) of 0.5 mm in the bending test (Technical Committee CEN/TC 229, 2005), were evaluated. Consistent relationships between the impact test parameters and those obtained from static bending test were found; as the static residual stress increases the total impact energy (E_T) increases and the impact crack growth rate (V_C) decreases. Additionally, the residual stresses ratio f_{R3}/f_{R1} presented an inverse exponential tendency with V_C beyond the type of fiber incorporated in the concrete.

Recently, a parametric study was performed to evaluate the effect of specimen geometry and other test variables (J.C. Vivas, Isla, et al., 2021). Impact tests were done on specimens cast from the same concrete varying the span length between supports (240, 350 and 500 mm), the specimen width (70, 100 and 150 mm), the notch depth (10, 25 and 50 mm) and the projectile mass (5, 10 and 20 kg). In addition, to verify the effect of each variable on impact test results, a correction factor was proposed in order to enable the comparison of each parameter.

Despite these advances, it is known that the matrix strength can affect the fibers failure mechanism. In addition, and considering that most of concrete properties have historically been related with compressive strength, it is imperative to investigate the effect of this property on FRC impact response. Some researchers have already made progress on this issue. Banthia (Banthia, 1987) compared the response of two plain concretes, a normal strength (water/cement ratio 0.5) and a high strength concrete in which micro silica was incorporated (water/binder ratio 0.33). A single drop-weight impact test was used, with instrumentation in beams, supports and the projectile. The hypothesis was that the concretes with highest performance under static loads do not necessarily would be the most efficient under dynamic loads. The result was that both high resistance and normal concretes behaved similarly; it was also concluded that, although the concrete with higher static strength had higher impact strength, it was more fragile in relative terms, since, despite having a higher maximum impact load, the magnitude of fracture energy was lower. An important point was that the failure mechanism changed between both concretes, which was evidenced in fracture through the aggregates in the case of the high strength concrete.

Mindess and Zhang (Mindess & Zhang, 2009) studied steel and polypropylene FRC, with base concretes compressive strength of 60, 90 and 120 MPa. They implemented a drop-weight test on cylinders subjected to compression by impact. They found that under impact the FRC presents greater deformation than the plain concrete but it exhibits greater compressive strength and toughness, being the toughness increases generally greater than the strength increases. Their results also show that while in FRC with low content of polymeric fibers (0.5% by volume) the Dynamic Increase Factors (DIF) of resistance, at a height of fall of 500 mm, were reduced with the increase of compressive strength, the effect was opposite for FRC with twice of content (1% by volume) of steel fibers. However, for other heights of fall different behaviors were observed.

Yoo et al. (Yoo, Yoon, & Banthia, 2015) evaluated FRC with three levels of compressive strength (49, 90 and 180 MPa) and four content of steel fibers (0, 0.5, 1 and 2 % in volume) through the drop weight test in bending on prisms. A simple impact from two potential energies (40 and 100 J) was used. Maximum impact loads increase as the compressive strength grew, in addition, the flexural strength was less sensitive to deformation rate in concretes with greater compressive strength. It is evident the key role of matrix strength on the FRC performance, however, although most variables should improve, it will not necessarily occur for all concrete properties. Additionally, as is shown at aforementioned investigations, the behavior

could vary between different types of fibers, even for the same type of filament component material, between different contents of same fiber, or if the configuration of impact test is changed. This paper constitutes a first step to understanding the effect of the matrix strength on the impact behavior of FRC evaluated thorough the proposed test. The study was performed on three base concretes with water/cement ratios varying between 0.43 and 0.59, reinforced with a same type and dosage of a steel fibers, typically used in many FRC applications.

2. Description of the problem

To assess the impact resistance of FRC, a repeated drop weight of impact test method has been recently developed, which consider both the resistance at cracking and the performance in the cracked state. Having previously studied the ability of the method to evaluate the influence of the type and content of fibers and the class of FRC as well as the geometry of the test, it is necessary to study the effect of matrix compressive strength on FRC impact response. The ability to differentiate concretes with diverse strength levels, both at cracking and in cracked state, represent a key point for application of the method.

3. Methodology

3.1. *Impact test*

The implemented impact test was proposed by the authors (Juan C. Vivas et al., 2020a, 2020b). It consists in a repeated impacts test, which are applied through a 5 kg projectile on a prism of 150x150x300 mm, with a notch of 25 mm of depth which is done by sawn in the middle of the tensile face. The specimen is simply supported with a span length between supports of 240 mm. Figure 1 shows a flow chart of test procedure, including setup and measurement, Phase 1 (up to cracking) and Phase 2 (cracked state).

The application of successive impacts is done according two Phases, or test stages. In Phase 1 the first impact is provided from a height of fall (h) 100 mm respect to specimen upper face, the subsequent impacts are applied increasing the height (Δh) 50 mm between each of them, the stage ends when appear a crack which is detected like will be explain ahead. Later the Phase 2 starts, in which, unlike the previous one, three impacts are applied in each height level, being the initial h level equal to 100 mm, in this case the subsequent increments Δh are 100 mm, the twice of previous Phase.

Along the test, after each impact, the crack opening (COD) is measured at 120 mm below the top face of the specimen, this is approximately 5 mm above the notch. For this, a digital microscope (Dino-Lite Premier AM4113T) is used; this device is supported and fixed to the test machine by mean a magnetic base and enough separate of specimen to avoid impact; the microscope is located 80 mm from the lateral surface specimen and the used magnification varies between 10x and 20x. Combining the measured COD and successive impacts height register, the named *"impact curve"* is obtained, this is the main obtained result from test, which the variation of accumulated potential energy (E*) as a function of the crack opening is plotted (E* versus COD). The potential energy is calculated as m.*g*.h, where *g* is the acceleration of gravity. Friction losses are not considered in this case since previous studies (J. Vivas, 2019) revealed a negligible influence of friction on results of this type of test (with a repeated impact pattern). The E* is the potential energy algebraic sum of impacts prior to certain point of test. The end of Phase 2, and test, was established for a COD greater than 3 mm.

The resulting test parameters used in the analysis are summarized as follows. From Phase 1, the Cracking Energy (E_C), which is the cumulated energy up to the appearance of the first crack and the opening of that initial crack (COD_C). From Phase 2 are obtained: E_P which is the accumulated energy after cracking until end of test, and V_C which is the rate of cracking calculated as inverse of slope of the chord in the impact curve between COD equal to 0.5 and 2.5 mm, expressed in μm/J. The total energy (E_T), calculated as $E_C + E_P$, represents a global parameter of the test. Setup, machine, devices used in the test and other details can be found in the cited papers (J. Vivas, 2019; Juan C. Vivas et al., 2020a, 2020b). A recent paper (J.C. Vivas, Zerbino, Torrijos, & Giaccio, 2021) includes an statistical analysis of the method, discussing variability aspects of the results and the minimum number of specimens recommended to achieve a enough confidence level.

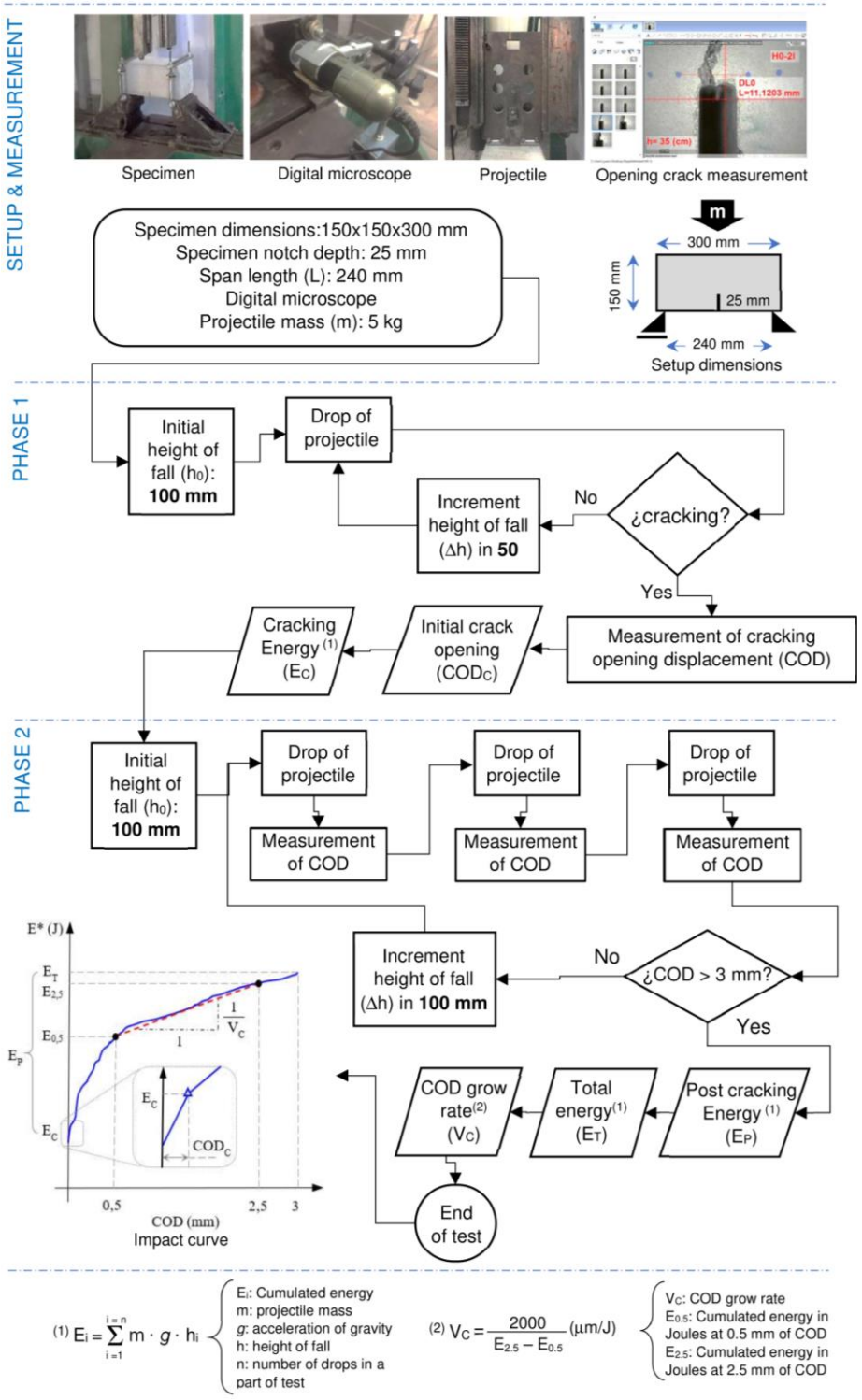

Figure 1. Impact test procedure.

3.2. *Materials and mixtures*

Three FRC (named H1, H2 and H3) incorporating 30 kg/m^3 of hooked-end steel fibers were prepared, the chosen fiber (see Figure 2) is low carbon steel kind, it has semi-circular section (1 mm diameter) and 50 mm of length. The tensile strength is greater than 1100 MPa.

Figure 2. Employed fiber.

The mixtures were prepared with 955 kg/m^3 of siliceous natural sand, 978 kg/m^3 of granitic crushed stone of 19 mm maximum size and 169 liters/m^3 of water. In each concrete a different content of CPN50 cement were incorporated (Instituto Argentino de Racionalización de Materiales, 2000), 280, 330 and 380 kg/m^3 for H1, H2 and H3, resulting concrete mixtures with water/cement ratios equals to 0.59, 0.50 and 0.43 respectively. A small dosage (<0.08% of weight of cement) of a high-range water reducer admixture was incorporated, with the aim to achieve the slumps around 10±1cm.

Three prisms of 150x150x600 mm and three cylinders of 100x200 mm were cast with each FRC. All specimens were compacted on vibrating table, unmolded after 24 hours and cured in moist room, for operational reasons, for one year. Then, they remained in laboratory environment for two weeks, to avoid alterations on results due to variations in the moisture content of specimens, and finally the static tests for FRC characterization and the impact tests were performed. The compressive strength and the elastic modulus were measured according to ASTM C39 and C469 standards (American Society for Testing and Materials, 2003, 2006), while the flexural tests were performed based on EN14651 standard (Technical Committee CEN/TC 229, 2005).

Table 1 presents the static characterization results of the three FRC. Notice that compressive strength (f'c) variation between the three concretes is near 11 MPa and, particularly, that concrete H3 is a high resistance concrete (f'c > 60 MPa). As expected, the elastic modulus (E) increased with the f'c. In the case of static bending test, as indicated in EN14651 standard, the first crack resistance (f_L) and residual stresses f_{R1} y f_{R3} calculated at 0.5 and 2.5 mm of crack mouth opening displacement (CMOD) are given. Complementarily, and considering that the stress-CMOD curves shows some slight initial hardening response, the maximum nominal stress (f_{max}), from the maximum load was also calculated and included.

As in the case of the modulus of elasticity, f_{max} and f_L increased as compressive strength increases. Regarding the residual capacity and FRC classes, following the *fib* Model Code 2010 (International Federation for Structural Concrete (fib), 2012), concretes H1, H2 and H3 can be classified as 3c, 4c and 4c respectively, which indicates that they show a post-cracking behavior where the residual capacity remains quite constant during CMOD increases. As can be seen in Figure 3, where the mean curves from three prisms of each FRC are plotted, there is a small increase in residual capacity for CMOD between 1 and 2 mm and later a softening tendency appears.

When analyzing Table 1, it is interesting to observe that, although the compressive strength increment from 44 to 67 MPa is clear, from the residual strength point of view, used for FRC classification, the mixtures practically correspond to a same FRC class; as exception, there is only a very small increase in f_{R1} in H3 but similar f_{R3}/f_{R1} ratio were found for the three FRC (the definition of Class "c" corresponds to $0.9 < f_{R3}/f_{R1} < 1.1$).

Table 1. Static characterization of concretes.

Concrete	Compression		Bending				
	f'c (MPa)	E (GPa)	f_{max}	f_L	f_{R1}	f_{R3}	f_{R3}/f_{R1}
			(MPa)				-
H1	44.2	42.2	5.2	4.9	3.8	3.5	0.92
H2	55.2	48.7	5.5	5.3	4.1	4.4	1.07
H3	67.1	49.7	5.9	5.5	4.5	4.5	0.99

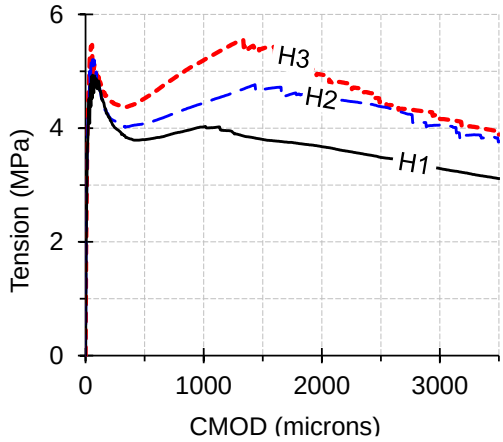

Figure 3. Mean Nominal Stress-Crack Mouth Opening Displacement (CMOD) curves, obtained from static bending test according to EN14651 standard.

4. Impact test results

For each FRC, 6 impact tests were carried out, using the resulting halves from static bending tests. From a variability study of the method it was found that this amount of specimens is enough for obtain the mean values of main parameters with an error lower than 15 % with a confidence level of 90 %, which are typical values accepted for FRC (J.C. Vivas, Zerbino, et al., 2021).

As mentioned in previous section, the main product of this test is the impact curve, which is the graphical representation of the crack opening (COD) versus the cumulated energy (E*). Figure 4 shows the individual impact curves of all specimens of three concretes included in this paper, each symbol corresponds to the application of an impact, and lines without symbols are the mean curves for each case (H1, H2 and H3). It can be appreciated that the variability of FRC curves was affected by the strength level of concrete. The smaller dispersion occurred for the concrete with lowest strength (H1: Figure 4 left), the dispersion was greater in the H2 and H3 (Figure 4 center and right) almost similar between them. In all cases an acceptable variability was observed which is in accordance with typical results of FRC, not only when considering the differences usually found in the residual capacity in static bending tests, but also when comparing the behavior of identical impact tests applied on FRC elaborated with 25 and 50 kg/m^3 of the same fibers (Juan C. Vivas et al., 2020a).

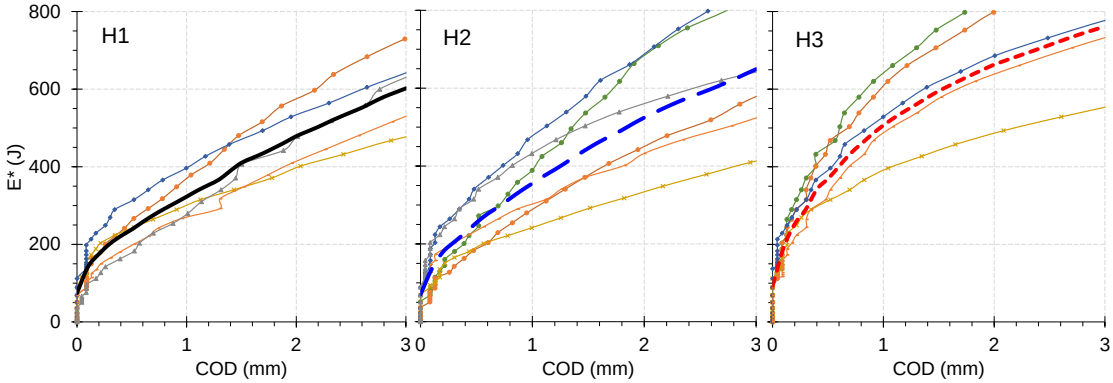

Figure 4. Individual impact curves of FRC. Each symbol represents an impact.

The mean impact curves obtained from each FRC are compared in Figure 5. As expected, the cumulated energy was greater as concrete strength increases. It can be seen that the shape of curve changes with the compressive strength of concrete. FRC H1 and H2 showed a clear linear behavior after cracking, approximately from COD greater than 0.4 mm. The high-strength concrete H3, initially less linear, becomes it after COD = 1.5 mm onwards. It can be noted that, despite the mentioned differences, in the last third of test for COD between 2 and 3 mm, the slopes of the impact curves were approximately equal.

The above observation suggests that the reduction in concrete water/cement ratio, which results in the increase in the matrix strength, benefited the adherence between the fiber and the matrix, improving the mechanical anchored of fibers and delaying the hook deformation and sliding of them. But once the hooks have been straightened and fibers slide occurs, the impact behavior of all concretes is almost similar.

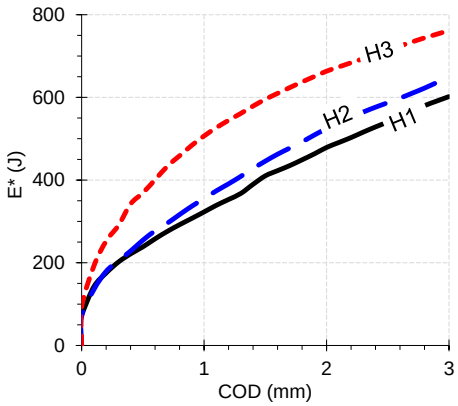

Figure 5. Mean impact curves from H1, H2 y H3.

A summary of impact parameters mean values from the three concretes is presented in Table 2. Some of these results are compared in Figure 6, the E_C and E_P energies (referred to left axis) and the V_C growth rate (referred to right logarithmic axis) are shown. The vertical lines indicate maximum and minimum values of each variable.

It can be observed that the cracking energy (E_C) remained practically constant in H1 and H2, while in H3 it increased approximately 20 %. In previous papers (Juan C. Vivas et al., 2020a) it was suggested that this variable depends on the matrix strength, this result reinforces that idea. However, it is clear that the improvements in E_C are evident from significant compressive strength increases (> 50%) and even so, the increase in this energy (E_C) was not proportional to f'c increase. In this case, although the resistance of H3 was 51 % higher than H1, the E_C only increased 21 %.

Table 2. FRC impact results.

Concrete	E_C (J)	COD_C (μm)	E_P (J)	V_C (μm/J)	E_T (J)
H1	96	69	530	7,0	625
H2	87	64	585	6,8	671
H3	116	42	665	6,2	782

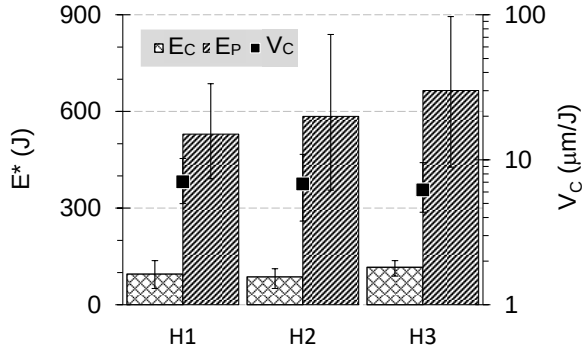

Figure 6. Impact parameters of H1, H2 and H3.

The first crack opening (COD_C) decreased as the compressive strength increased, although in other studies this parameter has been very unstable (high variability and unclear trend), its behavior was very reasonable in this research. As it was mentioned, the observed trend from this variable may be due to the fiber-matrix bond improvement as matrix strength increases. It is important to note that the reduction of COD_C between H1 and H2 concretes was small (7 %) while H3 decreased by almost 40 % respect to H1. Post-cracking energy (E_P) increased linearly with the compressive strength growth and in this case the improvement was proportional to f'c increase, approximately 5.5 J/MPa. The E_T (total energy) also increased as concrete compressive strength growth, very slightly between H1 and H2 (7 %) and 25 % between H3 compared to H1.

Finally, as compressive strength increases the COD growth rate (V_C) only decreased slightly and it can be considered practically constant. Possibly this behavior is due that once the bonding bridge fiber-matrix is broken and the fiber hook straightened, the crack opening only depends of fiber content, and therefore of number of filaments present in the fracture plane. In this case, it is presumed that this quantity would be constant in all concretes (H1, H2 and H3) as the three FRC were prepared with the same fiber content (30 kg/m^3). Consequently, and based on previous studies (Juan C. Vivas et al., 2020a), it is assumed that this parameter basically depends on the type and content of fibers used. This fact increases the advantages of the use of this parameter as means that the observed impact behavior for a same type and content of fibers can be assumed to be valid for a wide range of concrete compressive strengths, for instance, in this case, between 43 and 67 MPa.

5. Conclusions

Employing a repeated projectile drop-weight impact test three Fiber Reinforced Concretes (FRC) with the same content of hooked-end steel fibers but with different compressive strength were evaluated. The main conclusions are summarized following:

1. Concrete compressive strength affects the impact behavior of FRC and the used test can differentiate its influence;
2. Concrete strength growing improves the impact performance before and after cracking, which is evidenced in increases of cracking energy (E_C), post-cracking energy (E_P) and total energy (E_T);
3. The cracking energy (E_C) improvement was more evident in the case of high-strength concrete;
4. The most beneficed parameters by the strength increase were post-cracking energy and total energy (E_P and E_T), they grew up to 25 % due 50 % increase in concrete compressive strength;

5. Contrary to other parameters, the COD growth rate (V_C) remained practically constant despite the increase in static strength. These results indicate that the impact behavior for a same type and content of fibers can be assumed to be valid for a wide range of concrete compressive strengths.

Although the above conclusions are novel and interesting, must be clarified that arise from the evaluation of concretes reinforced with 30 kg/m^3 of hooked-end steel fibers and compressive strengths between 43 and 67 MPa. These results may vary and should be confirmed for other types and contents of fibers. Therefore, the effect of concrete static strength on FRC impact behavior still represents an area that needs to be studied.

Author contributions: Juan Carlos Vivas. Methodology, Validation, Formal analysis, Investigation, Writing – original draft. Raúl Zerbino: Conceptualization, Methodology, Formal analysis, Visualization, Writing – review & editing, Supervision.

Funding: not applicable.

Acknowledgments: the authors thank the support of LEMIT-CIC and funding from CONICET PIP112-20150100861 and UNLP 11/I244 projects.

Conflicts of interest: not applicable.

References

ACI Committee 544. (1999). *Measurement of Properties of Fiber Reinforced Concrete 544.2R-89*. *ACI* (Vol. 544.2R). Retrieved from http://civilwares.free.fr/ACI/MCP04/5442r_89.pdf

ACI Committee 544. (2017). *Report on Measuring Mechanical Properties of Hardened Fiber Reinforced Concrete*. *ACI 544.9R-17*.

American Society for Testing and Materials. ASTM C 39M (2003), Standard Test Method for Compressive Strength of Cylindrical Concrete Specimens (2003).

American Society for Testing and Materials. (2006). ASTM C 469 – 02 Standard Test Method for Static Modulus of Elasticity and Poisson ' s Ratio of Concrete. *Annual Book of ASTM Standards*, *i*, 2–6.

Banthia, N. P. (1987). *Impact Resistance of Concrete*. The University of British Columbia.

Instituto Argentino de Racionalización de Materiales. NORMA IRAM 50000 - Cemento para uso general (2000).

International Federation for Structural Concrete (*fib*). (2012). Model Code Volume 1.

Mindess, S., & Zhang, L. (2009). Impact resistance of fibre-reinforced concrete. *Proceedings of the Institution of Civil Engineers: Structures and Buildings*, *162*(1), 69–76. https://doi.org/10.1680/stbu.2009.162.1.69

Sateshkumar, S. K., Awoyera, P. O., Kandasamy, T., Nagaraj, S., Murugesan, P., & Ponnusamy, B. (2018). Impact resistance of high strength chopped basalt fibre-reinforced concrete. *Revista de La Construccion*, *17*(2), 240–249. https://doi.org/10.7764/RDLC.17.2.240

Technical Committee CEN/TC 229. EN 14651:2005 Test method for metallic fibered concrete - Measuring the flexural tensile strength (limit of proportionality (LOP), residual) Méthode (2005).

Ulzurrun, G., & Zanuy, C. (2017). Flexural response of SFRC under impact loading. *Construction and Building Materials*, *134*, 397–411. https://doi.org/10.1016/j.conbuildmat.2016.12.138

Vivas, J. (2019). Ensayo para el estudio de la resistencia al impacto de hormigones con fibras. In *Jornada de Jóvenes Investigadores en Tecnología del Cemento y Hormigón* (pp. 5–8). La Plata, Argentina: LEMIT. Retrieved from http://www.lemit.gov.ar/documentos/JJI_TCH_2019_actuales_investigaciones_tecnologia_cemento_hormigon_argentina_memorias_1

Vivas, J.C., Isla, F., Torrijos, M. C., Giaccio, G., Luccioni, B., & Zerbino, R. (2021). Drop-Weight Impact Test for Fibre Reinforced Concrete: Analysis of Test Configuration. In *RILEM-fib XI International Symposium on Fibre Reinforced Concrete*.

Vivas, J.C., Zerbino, R., Torrijos, M. C., & Giaccio, G. (2021). A Test Procedure for Evaluating the Impact Behaviour of Fibre Reinforced Concrete. *Materials and Structures.*

Vivas, Juan C., Zerbino, R., Torrijos, M. C., & Giaccio, G. (2020a). Effect of the fibre type on concrete impact resistance. *Construction and Building Materials*, *264*, 120200.

Vivas, Juan C., Zerbino, R., Torrijos, M. C., & Giaccio, G. M. (2020b). Impact response of different classes of fibre reinforced concretes. In P. Serna, A. LLano Torre, J. Martí Vargas, & J. Navarro-Gregori (Eds.), *RILEM-fib X International Symposium on Fibre Reinforced Concrete* (pp. 189–198).

Yoo, D. Y., Yoon, Y. S., & Banthia, N. (2015). Flexural response of steel-fiber-reinforced concrete beams: Effects of strength, fiber content, and strain-rate. *Cement and Concrete Composites*, *64*, 84–92. https://doi.org/10.1016/j.cemconcomp.2015.10.001

Yu, R., Van Beers, L., Spiesz, P., & Brouwers, H. J. H. (2016). Impact resistance of a sustainable Ultra-High Performance Fibre Reinforced Concrete (UHPFRC) under pendulum impact loadings. *Construction and Building Materials*, *107*, 203–215. https://doi.org/10.1016/j.conbuildmat.2015.12.157